International Journal of Applied Power Engineering (IJAPE)
Vol. 15, No. 1, March 2026, pp. 141~152
ISSN: 2252-8792, DOI: 10.11591/ijape.v15.i1.pp141-152

ANFIS-MPPT based PMSG-wind turbine interfaced with water pumping and battery management systems for optimal power flow and energy management

Saritha Kandukuri[1], Ram Dulare Nirala[1], Sivaprasad Kollati[2], Tata Himaja[3], Durga Bhavani Adireddy[4]
[1]Department of Electrical Engineering, Ekalavya University, Damoh, India
[2]Department of Electrical and Electronics Engineering, Godavari Global University, Rajahmundry, India
[3]Department of Electrical and Electronics Engineering, Aditya University, Surampalem, India
[4]Department of Electrical and Electronics Engineering, Vignan's Institute of Engineering for Women, Visakhapatnam, India

Article Info

Article history:

Received Oct 22, 2024
Revised Oct 30, 2025
Accepted Nov 28, 2025

Keywords:

Fuzzy logic
PMSG
PV panel
Water pumping
WECS

ABSTRACT

This paper presents the adaptive neuro-fuzzy inference system-maximum power point tracking (ANFIS-MPPT) approach for optimizing power flow in a water system powered by a permanent magnet synchronous generator (PMSG)-wind turbine. The system uses a PMSG-based wind energy conversion system (WECS) with an ANFIS for MPPT, enabling efficient power extraction under variable wind conditions. A bidirectional SEPIC-Zeta converter interfaces a battery energy storage system (BESS) to regulate the DC-bus voltage and maintain continuous power supply to a three-phase induction motor driving the water pump. An artificial neural network (ANN)-based controller is used to manage the charging and discharging of the battery based on real-time voltage deviation. The entire system, including wind turbine, PMSG, converters, and intelligent control algorithms, is modeled and simulated in MATLAB/Simulink. Comparative analysis with conventional MPPT techniques highlights the superior performance of the proposed hybrid ANFIS-based control in terms of power flow regulation, voltage stability, and operational reliability. The results confirm that the proposed approach significantly enhances energy management and system resilience, making it suitable for standalone or remote water pumping applications powered by renewable energy sources.

Corresponding Author:

Saritha Kandukuri
Department of Electrical Engineering, Ekalavya University
Damoh, Madhya Pradesh, India
Email: mugatha.saritha@gmail.com

1. INTRODUCTION

Renewable energy technologies have become essential in solving global energy demands and environmental concerns. Among these, wind energy has gained significant attention recently because of its widespread availability and ability to reduce carbon emissions [1], [2]. The increasing penetration of wind energy in modern power systems presents various challenges, particularly in protection, control, and integration aspects [3], [4]. With the surge in wind turbine installations, to achieve higher energy efficiency, it is essential to improve the performance of wind energy conversion system (WECS), especially in terms of reliability, energy storage, and operational efficiency [5], [6]. Permanent magnet synchronous generators (PMSGs) have emerged as a preferred solution for medium as well as large-scale wind turbines, which offer high efficiency and a compact structure, low maintenance, and ability to operate without external excitation

systems [7], [8]. Compared to doubly fed induction generators (DFIGs), which involve slip-ring assemblies and exhibit greater copper losses and maintenance concerns [9], [10], PMSGs offer superior performance, particularly under fluctuating wind conditions [11].

However, the control and modeling of permanent magnet synchronous generator (PMSG)-based WECS is still complex due to nonlinear behavior, wind speed variability, and load changes [12]. Researchers have explored various control strategies to optimize the power extraction and ensure system stability [13]. Techniques such as discrete-time direct torque control [14], space-vector-modulated sensorless control [15], and model predictive control (MPC) for bidirectional converters have been investigated for improving system response [16].

Incorporating energy storage systems such as batteries into WECS is another crucial area of research [17]. Proper coordination between the generator, load, and storage units ensures uninterrupted power delivery, voltage regulation, and frequency support [18], [19]. Bidirectional converter configurations like SEPIC-Zeta play a key role in managing power flows between the generator, battery, and the load [20]. Furthermore, efficient control mechanisms using advanced control approaches like fuzzy logic and adaptive neuro-fuzzy inference system (ANFIS), and AI-based techniques have demonstrated promising results in enhancing microgrid resilience and load-following performance [21].

Despite these advancements, there remain significant gaps in the seamless integration of maximum power point tracking (MPPT), battery energy storage system (BESS), and intelligent control techniques in a unified system for applications such as water pumping [22], [23]. Specifically, most prior works lack comparative evaluations under dynamic wind conditions and do not fully exploit hybrid control schemes to manage both energy capture and storage [24], [25]. To address these limitations, the present work proposes an integrated control strategy using an ANFIS-based MPPT approach, supported by a bidirectional SEPIC-Zeta converter and a battery energy storage system (BESS). The proposed system targets a practical application: reliable water pumping using wind energy while ensuring voltage stability and optimized energy utilization under varying wind profiles.

The main contributions of this paper are: development of an ANFIS-based MPPT control for efficient power extraction from the wind turbine. Design and implementation of a power-sharing strategy between the PMSG, battery, and water pump. Integration of a fuzzy logic controller for BESS to manage power flow and support microgrid stability. Simulation-based validation of the proposed system's performance in terms of efficiency, voltage stability, and load support under fluctuating wind conditions.

The rest of the paper is organized as follows: Section 2 presents the proposed system configuration and control structure. Section 3 describes the modeling and methodology. Section 4 discusses simulation results and performance evaluation. Finally, Section 5 concludes the paper with key findings and suggestions for future work. In the future, the techniques and methodologies developed in this paper can serve as a foundational framework for advanced research in intelligent control, fault-tolerant design, and grid stability for renewable energy systems. They may also come in handy in hybrid energy systems where wind energy is integrated with solar or battery storage solutions, opening avenues for smarter and more resilient energy infrastructure.

2. SYSTEM DESCRIPTION

The block diagram of the proposed work is shown in Figure 1. It represents a PMSG-based wind energy conversion system integrated with intelligent control strategies. The wind turbine drives a PMSG, whose output is regulated by a machine-side converter using ANFIS-based MPPT to extract maximum power. The regulated DC output powers a three-phase induction motor through a motor pump inverter. A bidirectional SEPIC-Zeta converter, controlled by an ANN-based controller, manages battery charging and discharging based on system voltage and load demand. Pulse width modulation (PWM) generators control all converters and inverters, ensuring efficient power flow and system voltage stability throughout.

The proposed methodology involves the detailed modeling and simulation of a PMSG-based WECS integrated with intelligent control strategies for maximum power extraction and energy management. The system includes a back-to-back converter configuration, where the machine-side converter regulates the PMSG output and maintains the DC link voltage. An ANFIS-based MPPT algorithm is implemented to improve power capture under varying wind conditions.

The ANFIS controller uses wind voltage and current as inputs to generate control signals for the machine-side PWM generator. This intelligent method is compared with conventional MPPT algorithms like perturb and observe (P&O) and incremental conductance (INC) to validate its superiority in dynamic wind conditions. The regulated DC output feeds a load-side inverter that supplies power to a three-phase induction motor driving a mechanical pump. Power calculations based on voltage and current feedback determine the PWM signals for the inverter. To ensure power balance and DC link stability, a bidirectional SEPIC-Zeta

converter is interfaced with a battery storage unit. An artificial neural network (ANN) based controller governs the converter operation based on reference and actual voltage levels, generating precise PWM signals to control charging and discharging according to battery SOC and load demand.

The entire system is implemented in MATLAB/Simulink, where both standard components and novel algorithms are modeled to enable replication and further analysis. The selection of ANFIS for MPPT and ANN for energy management is justified based on their ability to adapt to nonlinear dynamics and improve control accuracy compared to traditional approaches. This methodology enables a reliable, efficient, and intelligent energy conversion system capable of addressing the operational challenges of modern wind-based renewable energy systems.

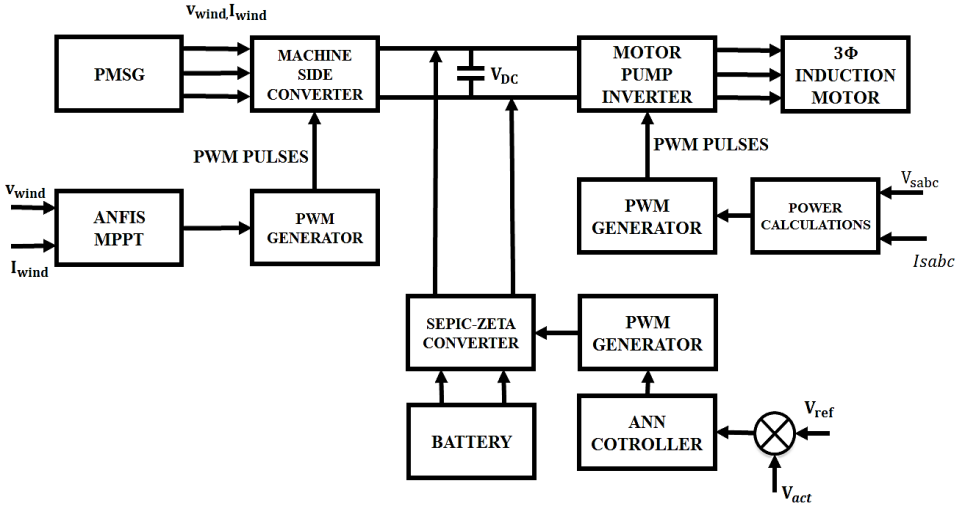

Figure 1. Block schematic for the suggested system

3. SYSTEM MODELLING

This section presents a detailed, step-by-step account of the system design and experimental procedures used in this study. Both standard and novel approaches are described with theoretical justifications and mathematical formulations to enable replication and validation.

3.1. Wind energy conversion systems

The wind energy conversion system (WECS) transforms wind energy into mechanical energy via a wind turbine, which is then converted to electrical energy using a generator. The inherent variability of wind introduces fluctuations in output frequency and voltage. These are stabilized using a power electronics interface consisting of a rectifier, DC-DC converter, and inverter to ensure grid-compatible output [23]. A wind turbine converts the kinetic energy of the wind into rotating motion. The generator converts mechanical energy into electrical energy. A rectifier converts AC voltage into dc. A manageable DC-DC converter suggests the maximum power point. All of these components work together to produce the wind power system. The symbol for generated power is (1).

$$P = \frac{1}{2}\rho A v^3 C_p(\lambda,\theta) R^2 V^3 \quad (1)$$

In which, P_m–power taken through wind turbine, ρ–air density, θ–pitch angle, R–blade radius, and V–wind speed. The ratio of tip speed in (2).

$$\lambda) = \frac{\Omega R}{V} \quad (2)$$

Here, R is rotor speed. Power coefficient (C_p) is given as (3) and (4).

$$C_p = \frac{1}{2}\left(\frac{116}{\lambda_1} - 0.4\beta - 5\right) e\left(\frac{-16.5}{\lambda_1}\right) \quad (3)$$

$$\lambda_1 = \frac{1}{\frac{1}{\lambda+0.089} - \frac{0.035}{\beta^3+1}} \tag{4}$$

Here, λ_1 is constant. TSR as tip-speed fraction represented as (5).

$$TSR = \frac{\omega_m R}{V} \tag{5}$$

Here, R-turbine radius and ω_m - mechanical angular speed in (6).

$$\omega_{opt} = \frac{TSR_{opt} V}{R} \tag{6}$$

The output torque is obtained from (2) and (6).

$$T = \frac{1}{2} \frac{\rho A C_{Pmax}}{\omega_{opt}} \left\{ \frac{R\omega_{opt}}{TSR_{opt}} \right\}^3 \tag{7}$$

3.2. Modelling of DFIG

The DFIG is modeled in the d-q reference frame, and both stator and rotor equations are provided. The voltage equations of stator as well as rotor are expressed as (8).

$$\begin{cases} v_{ds} = R_s i_{ds} + \frac{d}{dt}\phi_{ds} - \omega_s \phi_{qs} \\ v_{qs} = R_s i_{qs} + \frac{d}{dt}\phi_{qs} + \omega_s \phi_{ds} \\ v_{dr} = R_r i_{dr} + \frac{d}{dt}\phi_{dr} - \omega_r \phi_{qr} \\ v_{qr} = R_r i_{qr} + \frac{d}{dt}\phi_{qr} + \omega_r \phi_{dr} \end{cases} \tag{8}$$

Where the parts of the synchronised reference framework are designated as d as well as q, the stator and rotor are designated as s as well as r, the voltage is designated as v, the current is designated as i, the amount of flux is designated as ϕ, its frequency is designated as ω, and the resistance is designated as r.

The flux equations of stator as well as rotor are expressed as (9). Here, the inductance is defined as L and the mutual inductance as M.

$$\begin{cases} \phi_{ds} = L_s i_{ds} + M i_{dr} \\ \phi_{qs} = L_s i_{qs} + M i_{qr} \\ \phi_{dr} = L_r i_{dr} + M i_{ds} \\ \phi_{qr} = L_r i_{qr} + M i_{qs} \end{cases} \tag{9}$$

The mechanical equation for WECS based on DFIG is represented as (10).

$$j\frac{d\Omega}{dt} = T_a - T_{em} - f\Omega \tag{10}$$

When this generator's electromagnetic torque is given as T em, the coefficient of damping is given as f, the turbine's total inertia is given as J, and the DFIG speed is given as Ω. The DFIG electromagnetic torque, which is expressed as (11).

$$T_{em} = p\frac{M}{L_s}\left(\phi_{qs} i_{dr} - \phi_{ds} i_{qr}\right) \tag{11}$$

Where p denotes the pair of poles of the DFIG. On the stator side, the real and reactive power are expressed as (12).

$$\begin{cases} P_s = \frac{3}{2}\left(v_{ds} i_{ds} + v_{qs} i_{qs}\right) \\ Q_s = \frac{3}{2}\left(v_{qs} i_{ds} - v_{ds} i_{qs}\right) \end{cases} \tag{12}$$

3.3. SEPIC-Zeta converter

A dual-mode SEPIC-Zeta converter is proposed for bidirectional energy transfer and ripple current reduction. The converter allows step-up/step-down operation with improved efficiency using soft-switching techniques. Switches S1 to S4 control SEPIC or Zeta mode operation dynamically [25]. The converter reduces current stress and improves efficiency by eliminating inductor current fluctuations, enabling bidirectional operation and utilizing single PWM control for seamless mode transitions.

Step-up and step-down actions are possible independent of power translation guidance, as they were in the initial bidirectional SEPIC/Zeta converters. Due of the dualism of SEPIC and Zeta converters, a comparable procedure may be conducted in the bilateral orientation. When all accessory valves are switched out, the proposed converter performs similarly to the classic bidirectional SEPIC/Zeta converter due to the use of a single pulse width variation management. Without using interleaved approaches, the converter may eliminate inductor current fluctuations. In Figure 2, S1 is the primary switch in SEPIC operation, S2 is the synchronous rectifier, and S3 and S4 are the auxiliary switches. S1 conducts for the synchronous rectifier in ZETA operation, S2 is the primary switch, and S3 and S4 are the supplementary switches. The gentle current transition amongst switches is induced by La.

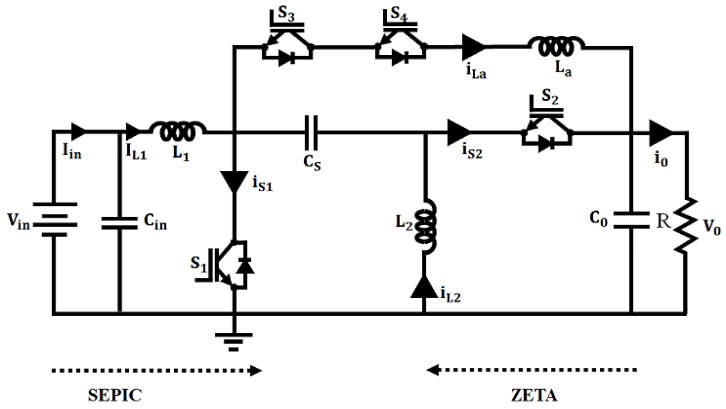

Figure 2. SEPIC-ZETA converter

3.4. ANFIS based MPPT

The ANFIS is employed to perform MPPT under varying wind conditions. The ANFIS receives the voltage and current from the wind energy system as inputs, while its output corresponds to the duty cycle of the DC–DC converter. The ANFIS model is shown in Figure 3. It takes three inputs—input voltage (V_{in}), input current (I_{in}), and wind speed—each processed through input membership functions (mf), followed by a rule layer that maps fuzzy rules based on combinations of the inputs. These are then passed through output membership functions and aggregated to produce a single output value, denoted as D.

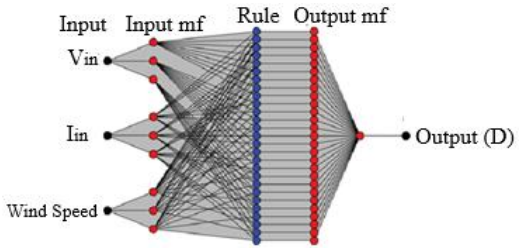

Figure 3. ANFIS model structure

The outputs are computed as linear combinations of the respective inputs, and the fuzzy rules can be formulated as follows:

- If $a = X_1$ and $b = Y_1$, then $F_1 = p_1a + q_1b + r_1$.
- If $a = X_2$ and $b = Y_2$, then $F_2 = p_2a + q_2b + r_2$.

Layer 1 contains adaptive nodes that produce membership values corresponding to linguistic terms, based on the input signals. These values are determined using a suitably parameterized membership function.

$$O_{1p} = \mu_{X_p}(a) = \frac{1}{1+\left|\frac{a-c_p}{x_p}\right|^{2y_p}} \quad (13)$$

Here, O_{1p} denotes the output of the p^{th} node in the initial layer, and $a$represents the input to that node. $X_i$refers to the linguistic label derived from $X = (X_1, X_2, Y_1, Y_2)$, which defines the fuzzy set. The parameters $\{x_p, y_p, z_p\}$ form the premise parameter set used to modify the shape of the membership function.

Layer 2 consists of fixed nodes, denoted by Π, which indicate the firing strength of each rule. In this layer, the output of every node is obtained by applying the fuzzy AND operation to all input signals.

$$O_{2p}= W_p = \mu_{Xp}(a)\ \mu_{Yp}(b), p = 1,2, \ldots \quad (14)$$

Layer 3 produces normalized firing strengths, where the output of the p^{th}node is calculated as the ratio of the firing strength of the p^{th}rule to the sum of the firing strengths of all rules.

$$O_{3p} = \overline{W_p} = \frac{W_p}{W_1+W_2} \quad (15)$$

Layer 4 outputs are calculated by the adaptive nodes depending on parameters utilizing.

$$O_{4p} = \overline{W_p}F_p = \overline{W_p}(i_p a + j_p b + k_p) \quad (16)$$

Here, $\overline{W_p}$ denotes the firing strength from the third layer and (i_p, j_p, k_p) are the nodes consequent parameter set. Layer 5 gives the overall output of ANFIS from the total of the inputs of nodes.

$$O_{5p} = \sum_i \overline{W_p}F_p = \frac{\sum_i W_p F_p}{\sum_i W_p} \quad (17)$$

The ANFIS controller generates the current, power of the PV system, and the duty cycle ratio of the converter as outputs. The input labels enable the ANFIS to produce the appropriate control command for the converter, ensuring effective power adaptation.

4. RESULTS AND DISCUSSION

The following outcomes are attained following completion of the anticipated tasks in the MATLAB simulation. Figures 4 and 5 show the motor side and battery side simulation diagram of a wind energy conversion system. The output from the wind turbine generator is fed through a rectifier and a DC-DC converter, where an inductor (L) helps control current ripple. Voltage and current compensators are used in the feedback loop to regulate battery charging by comparing the actual values with reference levels, ensuring stable and controlled energy storage.

Figure 6 shows the three-phase grid voltage waveform over a 1-second time interval. The waveform consists of three sinusoidal voltage signals, each phase-shifted by 120°, maintaining symmetry and balance throughout the duration. The voltage oscillates between ±1 V, indicating a well-regulated and stable grid connection suitable for power system operations.

Figure 7 presents the DC link voltage waveform over a time span of 1 second. The voltage remains relatively steady around 1100 V with minor ripples, indicating stable operation of the DC link in the power conversion stage. This stability is essential for maintaining consistent power flow between the AC-DC and DC-AC conversion processes in renewable energy systems.

Figure 8 illustrates the battery performance results, consisting of (a) battery voltage, (b) battery current, and (c) state of charge (SOC) waveforms over 1 second. Battery voltage remains stable around 12 V, indicating consistent voltage output during the simulation period. Battery current hovers close to zero, suggesting minimal charging/discharging activity, possibly indicating an idle or equilibrium state. Battery state of charge (SOC) stays constant at 60%, confirming no significant energy inflow or outflow during the simulation timeframe.

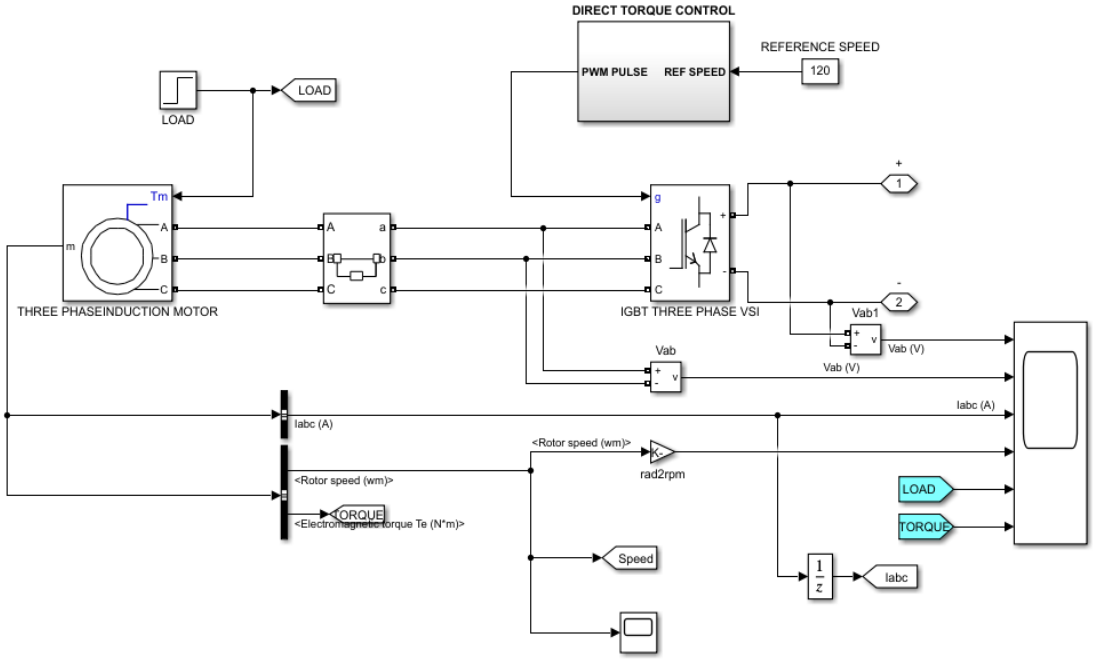

Figure 4. Motor side simulation diagram

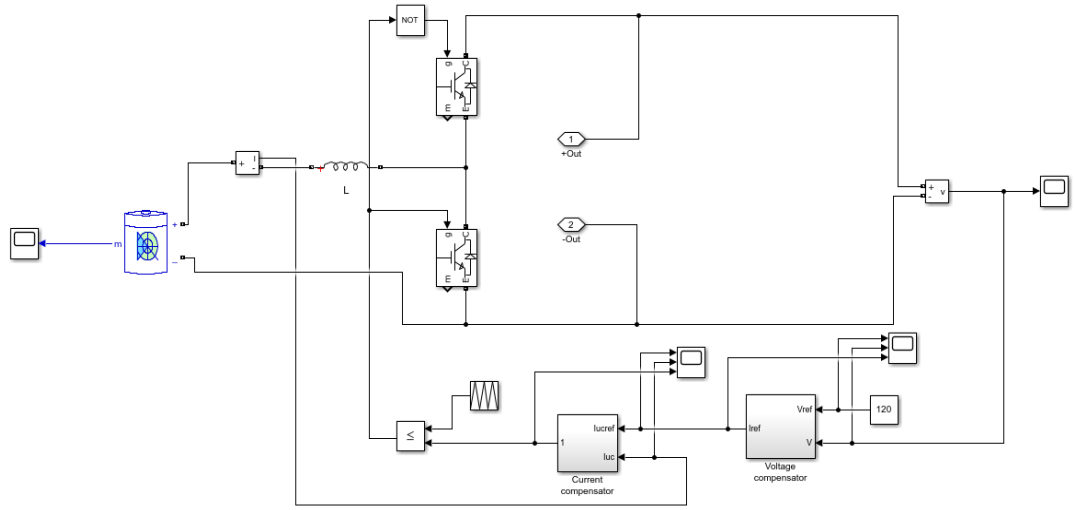

Figure 5. Battery side simulation diagram

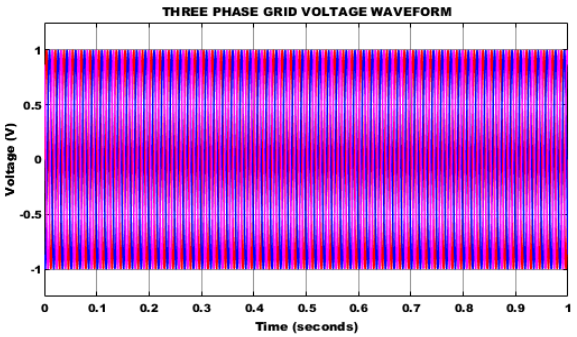

Figure 6. Grid voltage waveform

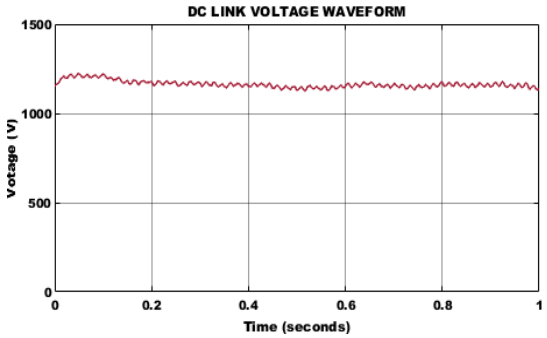

Figure 7. DC voltage waveform

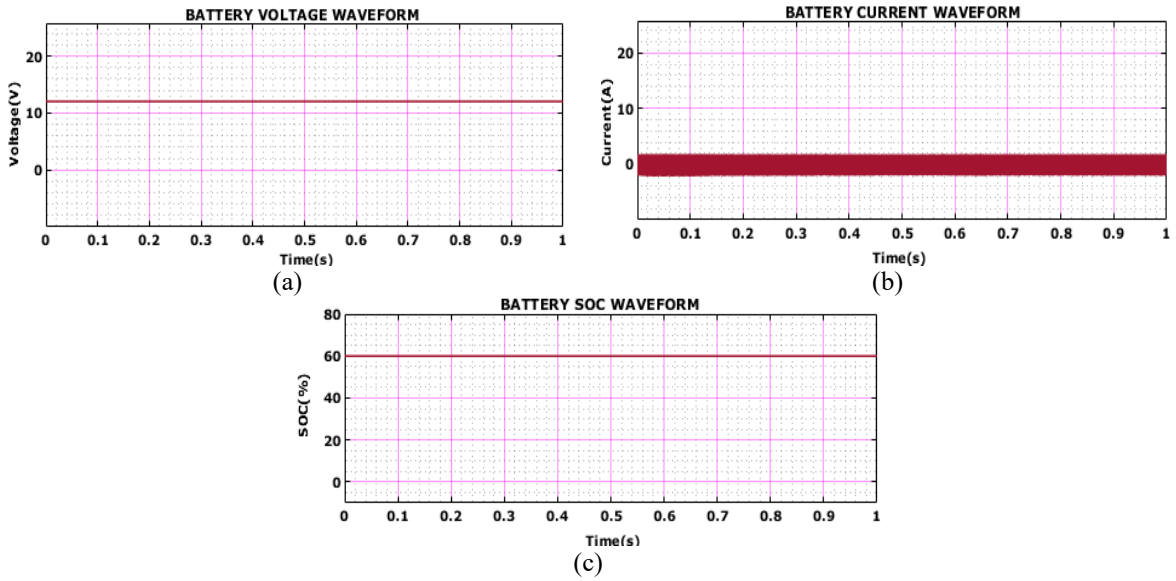

Figure 8. Battery results: (a) voltage, (b) current, and (c) SOC

Figure 9 illustrates the inverter line-to-line (L-L) voltage waveform, showing a consistent voltage range oscillating between approximately -1000 V and 1000 V. The waveform remains steady until around 0.55 seconds, after which noticeable distortions or disturbances appear, indicating a change in system conditions or load behavior. Figure 10 presents the motor load waveform, where the applied torque remains at 0 N·m until approximately 0.3 seconds. After 0.3 seconds, the torque steps up sharply to 2 N·m and stays constant for the remainder of the simulation period, indicating a sudden load application to the motor.

Figure 11 shows the motor current waveform, where the initial current reaches peak values close to ±600 A, indicating a high starting current during motor startup. As time progresses, the current amplitude gradually decreases and stabilizes, signifying the motor's transition to steady-state operation. Figure 12 displays the motor torque waveform, which begins at approximately 300 Nm and remains fairly steady with slight fluctuations until about 0.65 seconds. After 0.65 seconds, the torque decreases rapidly and eventually drops below zero, indicating a reversal or counter-torque applied to the motor. Figure 13 illustrates the motor speed waveform, which shows a smooth and continuous rise in speed from 0 to approximately 1350 RPM within the first 0.85 seconds. After 0.85 seconds, the speed begins to level off, indicating that the motor is approaching its steady-state operating condition.

Table 1 presents a comparison between the base system using P&O MPPT and the proposed system employing ANFIS MPPT in terms of efficiency, settling time, and harmonic distortion. The proposed ANFIS-based system demonstrates superior performance with higher MPPT efficiency (94%), reduced settling times, and significantly lower total harmonic distortion (THD) (2.1%) compared to the conventional P&O method.

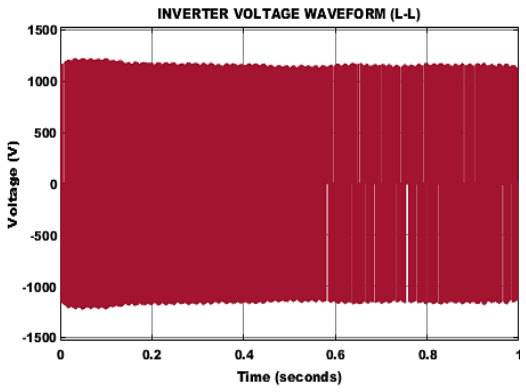

Figure 9. Inverter voltage waveform

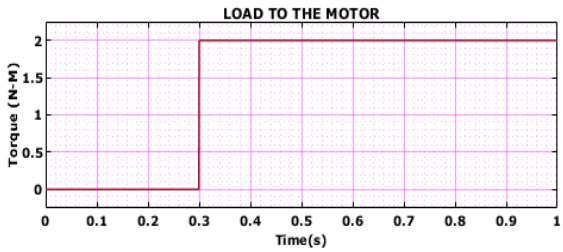

Figure 10. Motor load waveform

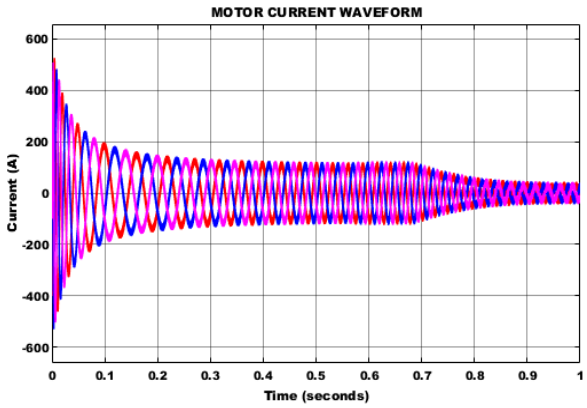

Figure 11. Motor current waveform

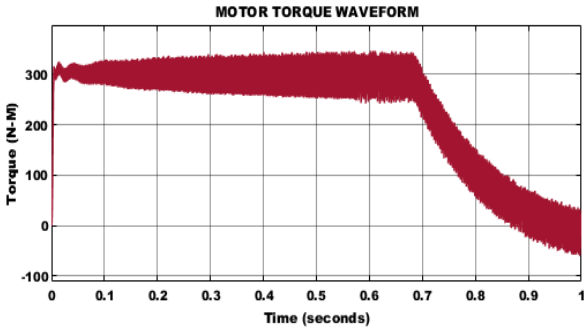

Figure 12. Motor torque waveform

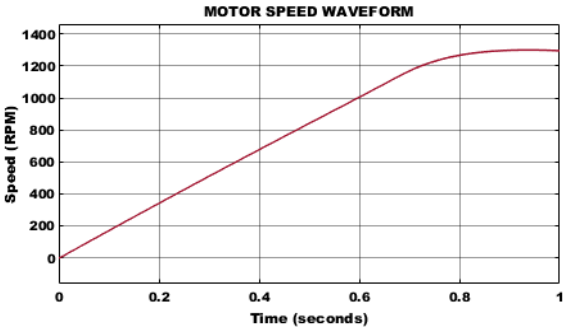

Figure 13. Motor speed waveform

Table 1. Comparison table

Parameter	Base system (P&O MPPT)	Proposed system (ANFIS MPPT)
Efficiency (MPPT)	88%	94%
Settling time (battery)	0.25 s	0.13 s
Total harmonic distortion (THD)	4.6%	2.1%
Settling time (output voltage)	0.21 s	0.10 s

5. CONCLUSION

This paper proposes an ANFIS-MPPT based PMSG-wind Turbine system integrated with water pumping and a SEPIC-Zeta bidirectional battery converter for optimal power flow and energy management. The ANFIS controller efficiently tracks the maximum power from the wind turbine, achieving an MPPT efficiency of 94%, outperforming the conventional P&O MPPT method which achieved only 88%. The proposed system significantly reduces power fluctuations and improves dynamic response, with battery settling time reduced from 0.25 s (P&O) to 0.13 s (ANFIS) and output voltage settling time improved from 0.21 s to 0.10 s. Additionally, the THD is minimized from 4.6% to 2.1%, ensuring higher power quality. The novel SEPIC-Zeta bidirectional converter contributes to efficient charging/discharging with enhanced voltage

gain and minimized losses. Simulation results using MATLAB 2021 and experimental hardware validation confirm the effectiveness of the proposed method. Future work will focus on real-time implementation under varying wind profiles and expanding the system to grid-connected and hybrid renewable energy applications.

FUNDING INFORMATION

The authors declare that no funding was received to support the research, or publication of this work.

AUTHOR CONTRIBUTIONS STATEMENT

This journal uses the Contributor Roles Taxonomy (CRediT) to recognize individual author contributions, reduce authorship disputes, and facilitate collaboration.

Name of Author	C	M	So	Va	Fo	I	R	D	O	E	Vi	Su	P	Fu
Saritha Kandukuri	✓	✓	✓	✓	✓	✓		✓	✓	✓		✓		✓
Ram Dulare Nirala		✓		✓	✓				✓			✓		
Sivaprasad Kollati	✓		✓	✓		✓			✓	✓		✓	✓	✓
Tata Himaja				✓	✓		✓			✓			✓	✓
Adireddy Durga Bhavani	✓			✓	✓			✓	✓	✓				✓

C : **C**onceptualization
M : **M**ethodology
So : **So**ftware
Va : **Va**lidation
Fo : **Fo**rmal analysis
I : **I**nvestigation
R : **R**esources
D : **D**ata Curation
O : Writing - **O**riginal Draft
E : Writing - Review & **E**diting
Vi : **Vi**sualization
Su : **Su**pervision
P : **P**roject administration
Fu : **Fu**nding acquisition

CONFLICT OF INTEREST STATEMENT

Authors state no conflict of interest.

DATA AVAILABILITY

The data that support the findings of this study are available from the corresponding author, [SK], upon reasonable request.

REFERENCES

[1] T. F. Megahed, E. F. Morgan, P. N. Timo, and M. Saeed, "Neural network predictive control for fault detection and identification in DFIG with SMES for low voltage ride-through requirements," *Ain Shams Engineering Journal*, vol. 15, no. 7, 2024, doi: 10.1016/j.asej.2024.102775.

[2] A. Watil, A. El Magri, R. Lajouad, A. Raihani, and F. Giri, "Multi-mode control strategy for a stand-alone wind energy conversion system with battery energy storage," *Journal of Energy Storage*, vol. 51, p. 104481, Jul. 2022, doi: 10.1016/j.est.2022.104481.

[3] M. M. Ahmed, H. M. Bawayan, M. A. Enany, M. M. Elymany, and A. A. Shaier, "Modern advancements of energy storage systems integrated with hybrid renewable energy sources for water pumping application," *Engineering Science and Technology, an International Journal*, vol. 62, p. 101967, Feb. 2025, doi: 10.1016/j.jestch.2025.101967.

[4] I. Matraji, A. Al-Durra, and R. Errouissi, "Design and experimental validation of enhanced adaptive second-order SMC for PMSG-based wind energy conversion system," *International Journal of Electrical Power & Energy Systems*, vol. 103, pp. 21–30, Dec. 2018, doi: 10.1016/j.ijepes.2018.05.022.

[5] C. A. Beltrán, L. H. Diaz-Saldierna, D. Langarica-Cordoba, and P. R. Martinez-Rodriguez, "Passivity-based control for output voltage regulation in a fuel cell/boost converter system," *Micromachines*, vol. 14, no. 1, p. 187, Jan. 2023, doi: 10.3390/mi14010187.

[6] Y. El Mourabit *et al.*, "Enhanced performance in PMSG-based wind turbine systems: experimental validation of adaptive backstepping control design," *Energies*, vol. 16, no. 22, p. 7481, Nov. 2023, doi: 10.3390/en16227481.

[7] A. Lozynskyy, T. Perzyński, J. Kozyra, Y. Biletskyi, and L. Kasha, "The interconnection and damping assignment passivity-based control synthesis via the optimal control method for electric vehicle subsystems," *Energies*, vol. 14, no. 12, p. 3711, Jun. 2021, doi: 10.3390/en14123711.

[8] S. Riffo, W. Gil-González, O. D. Montoya, C. Restrepo, and J. Muñoz, "Adaptive sensorless PI+passivity-based control of a boost converter supplying an unknown CPL," *Mathematics*, vol. 10, no. 22, p. 4321, Nov. 2022, doi: 10.3390/math10224321.

[9] S.-W. Lee and K.-H. Chun, "Adaptive sliding mode control for PMSG wind turbine systems," *Energies*, vol. 12, no. 4, p. 595, Feb. 2019, doi: 10.3390/en12040595.

[10] M. M. Rana, M. Uddin, M. R. Sarkar, G. M. Shafiullah, H. Mo, and M. Atef, "A review on hybrid photovoltaic – battery energy storage system: current status, challenges, and future directions," *Journal of Energy Storage*, vol. 51, p. 104597, Jul. 2022, doi: 10.1016/j.est.2022.104597.
[11] E. Sarmas, E. Spiliotis, V. Marinakis, G. Tzanes, J. K. Kaldellis, and H. Doukas, "ML-based energy management of water pumping systems for the application of peak shaving in small-scale islands," *Sustainable Cities and Society*, vol. 82, p. 103873, Jul. 2022, doi: 10.1016/j.scs.2022.103873.
[12] L. Guo, C. Xu, F. Zhang, F. Deng, X. Ai, and F. Xue, "Variable speed pumped storage units in China: current status and development," *Energy Reports*, vol. 13, pp. 2815–2828, Jun. 2025, doi: 10.1016/j.egyr.2025.02.017.
[13] P. Dey, M. Datta, N. Fernando, and T. Senjyu, "Fault-ride-through performance improvement of a PMSG based wind energy systems via coordinated control of STATCOM," in *2018 IEEE International Conference on Industrial Technology (ICIT)*, Feb. 2018, pp. 1236–1241, doi: 10.1109/ICIT.2018.8352355.
[14] A. A. Basheer, J. H. Jeong, S. R. Lee, and Y. H. Joo, "Power maximization using finite-control-set model predictive control strategy for wind turbine systems," *IEEE Journal of Emerging and Selected Topics in Industrial Electronics*, vol. 6, no. 1, pp. 238–247, 2025, doi: 10.1109/JESTIE.2024.3502658.
[15] S. Liu, H. Wu, T. Bosma, and X. Wang, "Impact of DC-link voltage control on torsional vibrations in grid-forming PMSG wind turbines," *IEEE Transactions on Energy Conversion*, vol. 39, no. 4, pp. 2631–2642, 2024, doi: 10.1109/TEC.2024.3394753.
[16] A. Ahmedi, M. Barnes, C. Ng, P. McKeever, and A. Egea-Àlvarez, "Mitigating converter thermal stress in PMSG wind turbines using enhanced control strategy and reduced order modeling," *IEEE Transactions on Energy Conversion*, vol. 40, no. 1, pp. 478–489, Mar. 2025, doi: 10.1109/TEC.2024.3449110.
[17] M. A. Mossa, R. A. Mohamed, and A. S. Al-Sumaiti, "Performance enhancement of a grid connected wind turbine-based PMSG using effective predictive control algorithm," *IEEE Access*, vol. 13, pp. 64160–64185, 2025, doi: 10.1109/ACCESS.2025.3557194.
[18] Y. Du *et al.*, "Deep reinforcement learning-based control scheme for performance enhancement of PMSG wind turbine with vienna rectifier," *IEEE Journal of Emerging and Selected Topics in Power Electronics*, vol. 13, no. 1, pp. 432–444, 2025, doi: 10.1109/JESTPE.2024.3452698.
[19] T. Zhang, S. Yang, Z. Hao, H. Ma, and B. Zhang, "An additional resonance damping control for grey-box D-PMSG wind farm integrated weak grid," *IEEE Transactions on Energy Conversion*, vol. 40, no. 1, pp. 270–283, 2025, doi: 10.1109/TEC.2024.3426050.
[20] B. Xu *et al.*, "A bidirectional integrated equalizer based on the sepic-zeta converter for hybrid energy storage system," *IEEE Transactions on Power Electronics*, vol. 37, no. 10, pp. 12659–12668, 2022, doi: 10.1109/TPEL.2022.3161984.
[21] A. A. Stonier *et al.*, "Fuzzy logic control for solar PV fed modular multilevel inverter towards marine water pumping applications," *IEEE Access*, vol. 9, pp. 88524–88534, 2021, doi: 10.1109/ACCESS.2021.3090254.
[22] A. Varshney, U. Sharma, and B. Singh, "An intelligent grid integrated solar PV array fed RSM drive-based water pumping system," *IEEE Transactions on Industry Applications*, vol. 57, no. 2, pp. 1818–1829, 2021, doi: 10.1109/TIA.2020.3045952.
[23] Z. Wang, R. Xie, J. Chen, T. Kang, and M. Zhang, "A flexible winding identification method utilizing self-attention and DNN for the double-suction centrifugal pump," *IEEE Transactions on Instrumentation and Measurement*, vol. 74, 2025, doi: 10.1109/TIM.2025.3554291.
[24] S. Orts-Grau *et al.*, "Photovoltaic water pumping: comparison between direct and lithium battery solutions," *IEEE Access*, vol. 9, pp. 101147–101163, 2021, doi: 10.1109/ACCESS.2021.3097246.
[25] C. Candelo-Zuluaga, J. R. Riba, A. G. Espinosa, and P. Tubert, "Customized PMSM design and optimization methodology for water pumping applications," *IEEE Transactions on Energy Conversion*, vol. 37, no. 1, pp. 454–465, 2022, doi: 10.1109/TEC.2021.3088674.

BIOGRAPHIES OF AUTHORS

Saritha Kandukuri is a research scholar, pursuing Ph.D. in electrical engineering at Eklavya University, Madhya Pradesh, India. She is working as an assistant professor in the Department of Electrical and Electronics Engineering at Godavari Institute of Engineering and Technology (Autonomous), Rajahmundry, Andhra Pradesh, India. She graduated in electrical and electronics engineering at Giet Engineering College, Rajahmundry, India. She graduated Master of Engineering in high voltage power systems at Godavari Institute of Engineering and Technology, Rajahmundry, Andhra Pradesh, India. She has been in the teaching profession for more than 8 years. She has presented 8 Scopus indexed papers in journals/conferences and 11 patents. Her main area of interest includes power systems and renewable energy systems. She can be contacted at email: mugatha.saritha@gmail.com.

Dr. Ram Dulare Nirala is an associate professor, HOD EC&EX Dept. Eklvaya University Damoh, MP, India. He graduated in electronics engineering from SGSITS Indore, MP, and did his master's from RGPV Bhopal, MP, in computer science engineering. He was awarded Ph.D. from Banasthali Vidhayapith, Banasthali Rajasthan, in image processing (enhancement techniques for dense foggy and hazy images). He has 25 years of teaching and research experience in computer and electronics engineering field. His expertises are in various engineering and technologies subjects particularly digital electronics, microprocessor, and communication network. He has one patent and 13 research papers published in national and international journals of repute. He also serves as research guide for the doctorate and master's degree programmes. He can be contacted at email: rdnirala@gmail.com.

Sivaprasad Kollati is working as an assistant professor in the Department of Electrical and Electronics Engineering at Godavari Institute of Engineering and Technology (Autonomous), Rajahmundry, Andhra Pradesh, India. He is a research scholar, pursuing Ph.D. in electrical engineering at Andhra University, Visakhapatnam, Andhra Pradesh, India. He is in the field of power electronics and renewable energy sources at Andhra University, Visakhapatnam, Andhra Pradesh, India. He graduated in electrical and electronics engineering at VIF College of Engineering and Technology, Hyderabad, India. He secured Master of Engineering in power electronics and electric drives at Pragati Engineering College, Surampalem, Andhra Pradesh, India. He has been in the teaching profession for more than 10 years. He has presented 11 Scopus-indexed papers in journals/conferences, one textbook, and 34 patents. His main area of interest includes power electronics and renewable energy systems. He can be contacted at email: ksivaprasad22@gmail.com.

Tata Himaja is working as an assistant professor in the Department of Electrical and Electronics Engineering at Aditya University, Surampalem, Andhra Pradesh, India. Her research interests include power electronics, smart grids, power systems, and electric vehicles. She can be contacted at email: himajatata@gmail.com.

Durga Bhavani Adireddy is currently working as an assistant professor in the Department of Electrical and Electronics Engineering at Vignan's Institute of Engineering for Women, Visakhapatnam, Andhra Pradesh, India. Her research interests include power electronics, renewable energy sources, power systems, and electric vehicles. She can be contacted at email: bhavani.adireddy@gmail.com.